Influence of wind angle incidence and architectural elements on the external pressure coefficient of hyperbolic paraboloid roofs

GUILHERME S. TEIXEIRA, MARCO D. DE CAMPOS
Institute of Exact and Earth Sciences
Federal University of Mato Grosso,
Av. Valdon Varjão, 6390, Barra do Garças, 78605-091, Mato Grosso
BRAZIL

Abstract: In the study of wind loads in buildings, the aerodynamics of roofs with parabolic shapes, which cause complex pressure distributions due to their sensitivity to wind, are often omitted and neglected by several codes and norms. In this way, computer simulations are a viable and reliable alternative. Here, wind action was considered in an innovative project composed of parabolic and circumferential generatrices: the *Church of Saint Francis of Assisi.* Designed by Brazilian architect Oscar Niemeyer in Belo Horizonte, Brazil, two paraboloid vaults and three circular arches of reinforced concrete composed its structure. This work generated great international recognition for the architect after 1943, as the design of the roofs did not require walls. For geometry modeling, *Autodesk AutoCAD* software was adopted, and the models were considered in a control volume. The simulations were performed using *Ansys Workbench* software and the *RNG K-Epsilon* turbulence model. The wind speed at different heights was calculated using the Power-law approximation. A basic wind speed of 30 m/s was adopted, and the mesh used was composed of tetrahedrons. To validate the methodology, different models with hyperbolic-paraboloid roofs from the literature were considered. In addition, the visualization of the flow around the geometry from the streamlines, the wind profile, and the analysis of the isobaric lines of the external pressure coefficients for different directions of incidence and architectural elements that make up the building were presented.

Key-Words: Wind action, parabolic roof, *Ansys*, pressure coefficients, computational method.

Received: July 28, 2021. Revised: April 22, 2022. Accepted: May 17, 2022. Published: June 30, 2022.

1 Introduction

Widely used in engineering and architecture are hyperbolic paraboloid roofs, especially in buildings with large spans in which the rooftop and wall constitute a single element. The arch axis is composed of a parabola, allowing for the construction of large spaces. This type of building is a specific class of laminar structures with double curvature that allows the design to carry forces either solely or predominantly through membrane forces such as uniform tension, compression, and shear through the thickness of the shell [1]. Arched roof structures often have a low permanent load and are wind sensitive with a small payload capacity [2]. Using a parabolic roof as a roof has the advantages of a harmonious shape, satisfactory strength performance, and easy construction.

However, some restrictions limit the use of these structures: the complexity of this type of project and the absence of mandatory norms for the structural project in the most different international codes. Thus, numerical and experimental experiments are the only way to study and investigate the wind-structure interaction in this geometry [3].

Among these, Rizzo and Sepe [4] explored the possibility of defining static pressure fields capable of reproducing the dynamic displacements of the cable network based on experimental wind tunnel tests on hyperbolic paraboloid roofs [5] and simplified pressure maps evaluated in Rizzo et al. [6]. The tests were carried out in a CRIACIV boundary layer wind tunnel in Prato, Italy, to determine the pressure fields for various angles of attack of the incident wind in different models of hyperbolic paraboloid roofs. Xu et al. [7] investigated the mechanical characteristics of the open hyperbolic-parabolic membrane structure under a wind load and the influences of wind directions and speeds on the mean wind pressure distribution. The wind load shape coefficients of constructions with an open hyperbolic-parabolic membrane were obtained from a series of numerical calculations and compared with values in the literature. Rizzo and Demartino [8] proposed a

modification of mean pressure coefficients on hyperbolic paraboloid roofs. *Singular value decomposition* (SVD) on data from wind tunnel tests applied to eight different geometries of buildings covered was used to obtain the pressure coefficients. Three wind incidence angles, 45° and parallel to downward and upward cables, namely, 0° and 90°, respectively, were investigated.

The mean pressure coefficients were modified using the superpositions of pressure for all eight geometries. To estimate the wind action and the vertical displacements of a cable net by FEM analyses, symmetrical and asymmetrical pressure coefficient modes were adopted. The results indicate that these load combinations allow for capturing large downward and upward displacements not accurately predicted using mean experimental pressure coefficients. Rong et al. [9] numerically simulated the wind pressure distribution on the roof of Wanda Ski Park, located in Harbin, China, comparing the mean wind pressure distribution data with the results of existing tests in wind tunnels. Based on the total pressure coefficients, they proposed an evaluation method where only the roof geometry and the wind incidence angle need to be known.

Many architects have used this type of construction, for example, in the restaurant of *Ciutat de Les Arts I Les Ciències* in Valencia, Spain, and the *Restaurante Los Manantiales* in Xochimilco, Mexico, designed by Felix Candela. Additionally, *Bosjes Chapel* by architect Coetzee Steyn in South Africa. In Brazil, one of the most representative examples is the *Church of Saint Francis of Assisi* by Oscar Niemeyer in Pampulha Modern Ensemble, Belo Horizonte, Brazil. The inclination of the roof and the repetition of a uniform motif on the main floor integrate itself magnificently with the simplicity and lack of pretension of already known buildings. Far from being a pastiche, the building maintains its contemporaneity and offers a plastic form. Its structure is composed of reinforced concrete arches forming two parabolic domes (Fig. 1). The use of this form allowed a single element to form the roof and walls. The bell tower and the marquee at the entrance appear as independent structures (Fig. 1).

In this work, the pressure coefficient with numerical tests on different geometries of hyperbolic paraboloid roofs was investigated considering different wind angles of attack as well architectural element influences (the bell tower and marquee).

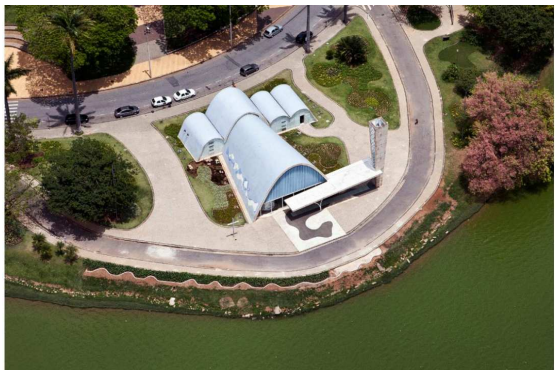

Fig. 1 Aerial photo of the Church of Saint Francis of Assisi [10]

2 Methodology

In this work, meshes and postprocessing were performed with *Ansys Workbench* software, and the simulations took place with the *CFX* solver. For geometry modeling, *Autodesk AutoCAD* software with dimensions proposed by Macedo [11] was used, as shown in Fig. 2a. According to Franke et al. [12], a control volume was used for low-rise buildings (i.e., H~B~L), whose adopted dimensions were as follows: length of 5H+L+15H, width of 5H+B+5H, and height of H+5H, dependent on the building height of (H = 9.16 m), length L of the building in the flow direction and width B (Fig 2c).

For the local refinement of the mesh, an influencing body with the following dimensions was used (Fig 2b): L for the length of the downstream region and half of this length upstream and, in addition, twice this dimension for the width and height [13].

The wind speed was estimated using the Power-law approximation with a height of 10 m.

Here, an unstructured mesh composed of tetrahedrons with curvature and capture proximities and three levels of refinement was used. The first level defines the dimensions of the elements in the fluid domain. The second and third levels, respectively, characterize the refinement of local (with the body of influence) and geometric faces that intercept the flow. In terms of advection, a *High-resolution scheme* was chosen in all applications [14].

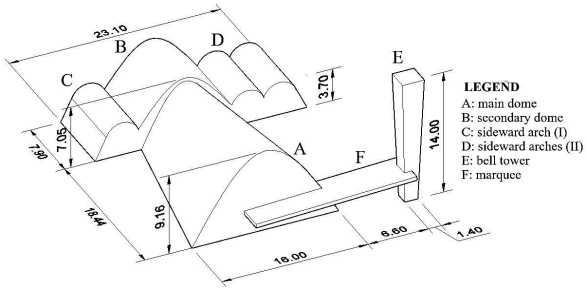

(a)

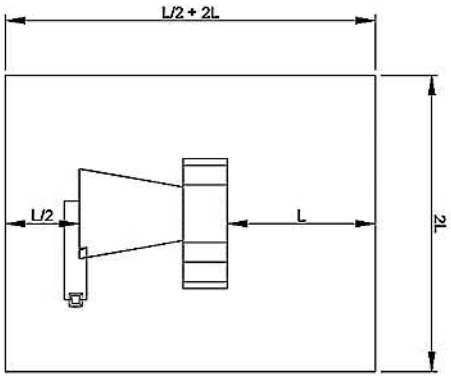

(b)

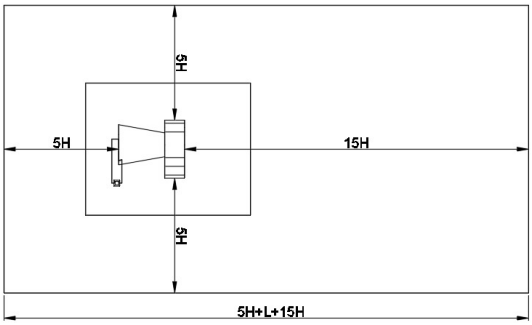

(c)

Fig. 2 (a) Dimensions and architectural components of the Church of Saint Francis of Assisi, (b) geometry and control volume, (c) geometry and body of influence

Using the residual root mean square (RMS) between subsequent iterations of a variable over all the domain's volumes, it is possible to estimate the iteration error present in codes that use iterative solvers. The convergence criterion for the simulations, in double precision, was defined as a root mean square residual target value of 1×10^{-4}. The maximum and minimum numbers of iterations were 400 and 500, respectively.

Using tetrahedral volumes, discretization was performed. In this case an unstructured mesh was used, considering its easy construction and that *CFX* in *Ansys Workbench* employs an unstructured code. Furthermore, the "*capture curvature and proximity*" tool, activated during all simulations, generated an adaptive process of the mesh elements close to the edges and curves of the adopted geometries. As a result, the stretching and compression of the tetrahedral mesh were avoided for high gradient regions. Finally, this resulted in a small truncation error [14].

To solve the governing equations of problems involving *Computational Fluid Dynamics* (CFD) and transform complex equations into algebraic equations, discretization is used. Faced with this, Franke *et al*. [14] recommend high-order schemes for discretizing advective terms. In this work, the advection scheme and numerical turbulence were high resolution. Table 1 depicts the boundary condition details.

The convergence analysis was performed according to the following criteria. The first is related to the residual RMS of the energy, mass, momentum, and additional turbulence equations due to the *RNG K-Epsilon* model. The second was the monitoring of mass conservation, given by the IMBALANCE monitor, which showed consistent values (<1%) according to [15].

Table 1. Boundary conditions and nondimensional parameters.

Condition		Parameters
Method of mesh		Tetrahedron
Capture curvature and proximity		On
Reference pressure		101325 [Pa]
Air temperature		25º [C]
Turbulence intensity		Medium (5%)
Flow regime		Subsonic
Inlet		$U/U_{ref} = (Z/Z_{ref})^{\alpha}$
Relative pressure of outlet		0 [Pa]
Wall (terrain)		Rough wall
Model wall roughness		Smooth wall
Roughness	*Application 1*	0.0025 [m]
	Applications 2 and 3	0.01 [m]
Reference height	*Application 1*	0.1 [m]
	Applications 2 and 3	10 [m]
Wind speed	*Application 1*	16.7 [m/s]
	Applications 2 and 3	30 [m/s]
Advection scheme		High resolution
Turbulence numeric		High resolution

3 Numerical applications

Application 1 (*Validation*): For the validation of the methodology, the external wind pressure results on hyperbolic paraboloid roofs for three wind directions were calculated. Hereafter, the results were compared with [4].

The model dimensions are defined in Fig. 3 and reported in Table 2 according to [4]; f_1 and f_2 denote the sag of the cable (upward curvature) and of the stabilising cable (downward curvature), respectively, H and h are the maximum and minimum height of the roof on the ground, respectively, and L is the dimension of the plan sides.

Table 3 shows the computational mesh applied to the domain.

Parameters such as the element quality, skewness, and orthogonal quality were estimated with special attention. The element quality describes the relationship between element area and border length (with recommended values close to 1).

Table 2. Dimensions of sample cases.

Sample	**H** [m]	**h** [m]	**f_1** [m]	**f_2** [m]	**L** [m]
1	0.2133	0.1333	0.0267	0.0533	0.8000
2	0.2666	0.1333	0.4440	0.0890	0.8000

Table 3. Results for *Models 1, 2, 3, 4, 5* and *6* with their respective quality metrics.

Model	*1*	*2*	*3*	*4*	*5*	*6*
Geometric configuration	1	1	1	2	2	2
Wind direction	0º	45º	90º	0º	45º	90º
Element size in the fluid domain (m)	0.07	0.1	0.08	0.1	0.1	0.1
Element size in the body of influence (m)	0.035	0.05	0.04	0.05	0.05	0.05
Element size on geometry faces (m)	0.005	0.01	0.005	0.01	0.01	0.02
Nodes	465186	190999	402417	177443	242653	126447
Elements	2571471	1066180	2207163	984627	1363700	712401
Element quality (average)	0.84401	0.84735	0.84260	0.84623	0.84851	0.85038
Skewness (average)	0.21802	0.21293	0.22013	0.21448	0.21095	0.20805
Orthogonal quality (average)	0.78080	0.78593	0.77867	0.78435	0.78792	0.79083

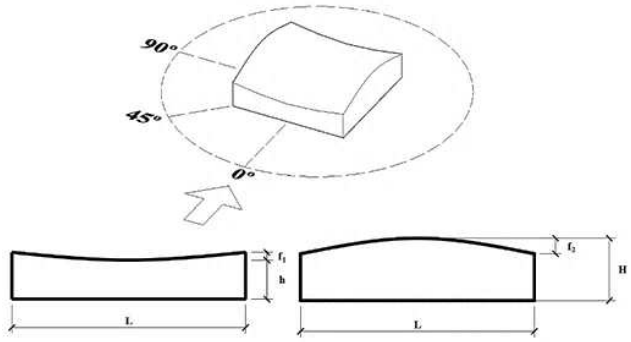

Fig. 3 Geometric characteristics of the model.

In turn, the skewness characterizes the proximity of the ideal geometry (in this case, the tetrahedron), the mesh cells, or faces (with recommended values between 0 and 0.5). Finally, orthogonal quality defines the element's orthogonality (with recommended values close to 1) [16].

To model the physical conditions, the wind profile was defined using the Power-law approximation for a reference height equal to 0.1 m, an exponent equal to 0.233, and a wind speed of 16.7 m/s, and for the terrain, the roughness adopted a value of 0.0025 m.

In general, the simulations showed good agreement in the distribution of the isobaric lines with the experimental samples. Considering a precision house, the best concordance, in absolute values, occurred in *Model 1* (Fig. 4). The highest discrepancy occurred at the midpoint of the left edge in *Model 2*, with a value of 0.4. The color hue represents the pressures that act on the surfaces corresponding to the pressure coefficient ranges: warm colors represent the overpressure regions, and the cold colors represent the suction regions indicating the detachment of the flow in the corners of the lateral faces of the geometry before reaching the cover. The results are presented in Table 4.

Then, to determine significant differences between the present work results and the literature, the *T-test* was used, considering a null hypothesis that the means are not different. Thus, considering a one-tailed distribution, *p-value*=0.42 was obtained for a critical *t*=1.72. As 0.42<1.72, it was possible to conclude that the difference between the mean values of *Cpe* is insignificant.

Application 2 (*External pressure coefficients for Church of Saint Francis of Assisi*): Here, the external pressure coefficients of the Church of Saint Francis of Assisi were acquired considering eight wind angles.

According to [17], a wind speed equal to 30 m/s was adopted. Thus, the directions of 0°, 45°, 90°, 135°, 180°, 225°, 270°, and 315° (Fig. 5) were simulated in different domains, and the data are presented in Table 5.

Considering an average height of the surrounding obstacles of 10 m, the exponent is equal to 0.25 for the power-law parameter [18]. The results showed how the pressures act on the structure, emphasizing paraboloid concrete covers (Fig. 6).

Directions 0° and 180° (*Models 7* and *11*) were those in which the fluid showed detachment from

the building at the corners of the main facades (Fig. 7), generating mostly suction zones on the roofs. The case at 0° presented a more intense peak in the main canopy bark (Cpe_{min}= -0.72).

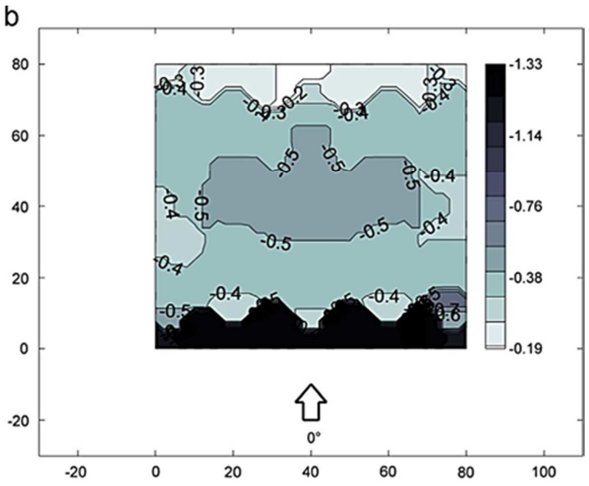

(a) [4]

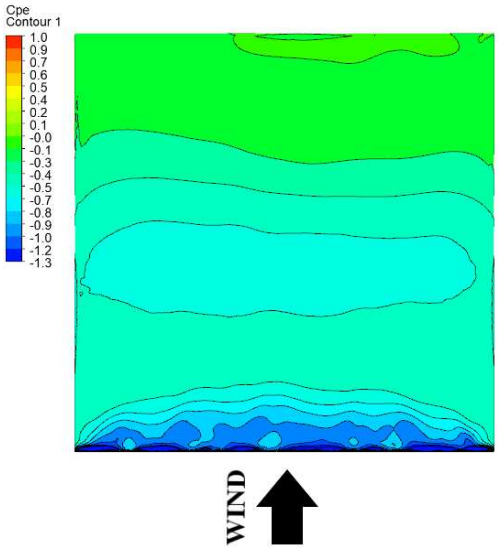

(b) Present work

Fig. 4 *Cpe* contours for *Model 1*.

Table 4. Pressure coefficients comparison.

Model	*1*		*2*		*3*	
	Cpe_{max}	Cpe_{min}	Cpe_{max}	Cpe_{min}	Cpe_{max}	Cpe_{min}
[4]	-0.2	-1.3	-0.2	-1.6	-0.8	-1.4
Present work	-0.2	-1.3	-0.3	-2.0	-0.7	-1.4
Difference	0.0	0.0	0.1	0.4	0.1	0.0
Model	*4*		*5*		*6*	
	Cpe_{max}	Cpe_{min}	Cpe_{max}	Cpe_{min}	Cpe_{max}	Cpe_{min}
[4]	-0.1	-0.9	-0.2	-1.8	-0.1	-1.2
Present work	-0.1	-1.0	0.0	-2.1	-0.1	-1.3
Difference	0.0	0.1	0.2	0.3	0.0	0.1

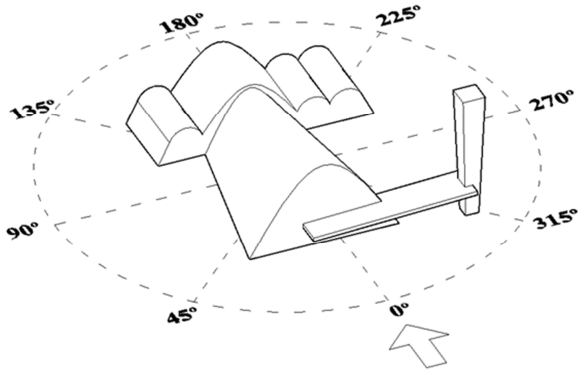

Fig. 5 Different angles of incidence of the wind in the *Church of Saint Francis of Assisi*.

For cases in which the wind directly or partially impinges on the parabolic roofs, the building presented suction peaks in the inflection region of the concrete shell and a clear separation between the suction and overpressure regions. In terms of higher suctions, *Model 4* (90°) stood out with Cpe_{min}= -1.86 (Fig. 8).

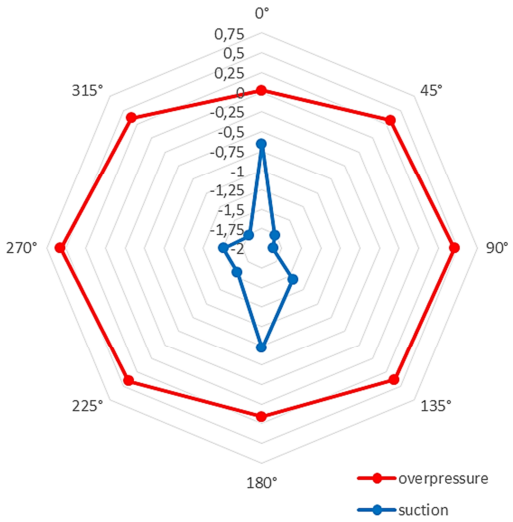

Fig. 6 Maximum and minimum *Cpe* for different angles of incidence of the wind (in absolute values).

Despite the significant similarity in the isobaric lines, no axes of symmetry were observed in the inclined roofs for cases of direct or partial incidence of the fluid.

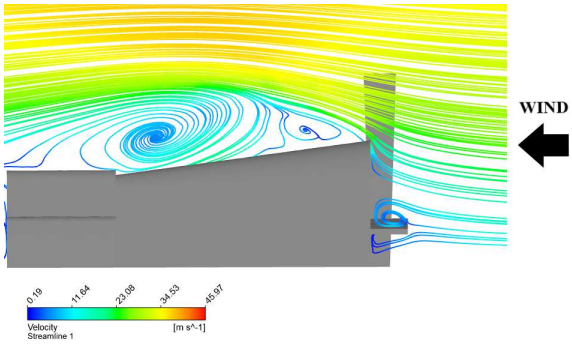

(a)

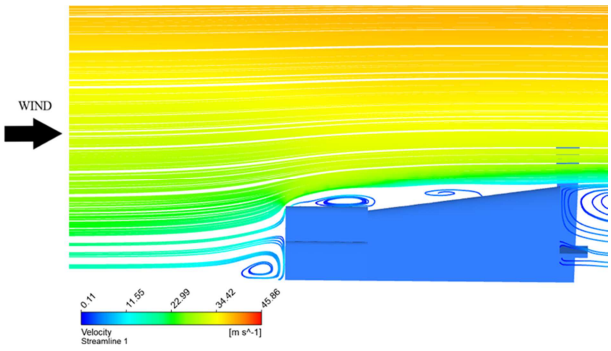

(b)

Fig. 7 Streamlines in a longitudinal plane for (a) *Model 7* and (b) *Model 11*.

Table 5. Results for *Models 7, 8, 9, 10, 11 and 12* with their respective quality metrics.

Model	*Wind direction*	*Nodes*	*Elements*	*Element quality (average)*	*Skewness (average)*	*Orthogonal quality (average)*
7	0º	118465	666741	0.82183	0.24691	0.75202
8	45º	147195	834265	0.81955	0.24946	0.74948
9	90º	109654	615181	0.82166	0.24747	0.75144
10	135º	140317	793734	0.82035	0.24854	0.75039
11	180º	119801	673748	0.82199	0.24660	0.75232
12	225º	144692	819670	0.81924	0.24989	0.74905
13	270º	123124	694732	0.82107	0.24804	0.75089
14	315º	138645	783688	0.82025	0.24876	0.75018

Application 3 (*Architectural elements influence*): Architectural and constructive elements, such as sun visor devices and projection in the structure, are relevant factors in the thermal comfort study and natural ventilation in buildings and their influence in this type of analysis. However, they can be neglected during the pressure coefficient analysis, going through simplifications.

This application analyzed the bell tower and marquee influence (E and F in Fig. 2a) present in the church architecture. The bell tower has the shape of an inverted pyramid trunk and contributes to supporting the marquee, which has a slight inclination. The elements are the only ones that have straight lines in their design, creating contrast between the circular and parabolic curves of the domes and sideward arches (Fig. 1). The 315° direction was chosen (Fig. 5) because, in this case, the fluid intersects two architectural elements before the building. These elements were disregarded in the simulation, and the results were compared with *Model 14*. The meshes were composed of 4.0 m tetrahedrons in the fluid domain, 2.0 m in the body of influence, and 0.5 m in the building faces. For this application 0.25 for the power-law parameter [18] was also adopted, and the terrain was defined as a rough wall with a roughness of 0.01 m. Table 6 presents the mesh results for these models with their respective quality metrics.

Model 15 presented a distribution of pressure coefficients in the coverage similar to *Model 14*; for the case of the complete model, the range was from -0.03 to -1.68, equivalent to -0.07 to -1.77 (Fig. 8(h)-(i)). The distinction of the main dome's overpressure and suction regions (A in Fig. 1) was conserved, and the suction peak occurred in the parabola inflection region for both cases.

The analysis of the interferences of the marquee and bell towers alone in the fluid flow allows the study of the slight difference in the results between these two simulations. Figure 9 presents the velocity contours parallel to the terrain at different levels (2 m, 3.5 m, and 5 m) intersecting the architectural elements (*Model 15*). On the first level (Fig. 9a), where the contour intersects the bell tower below the marquee, a large part of the fluid, including that near the bell tower, was at low speeds (approximately 14 m/s). This behavior is expected, given that for a height of 2 m, the power-law will return low values for the velocity component.

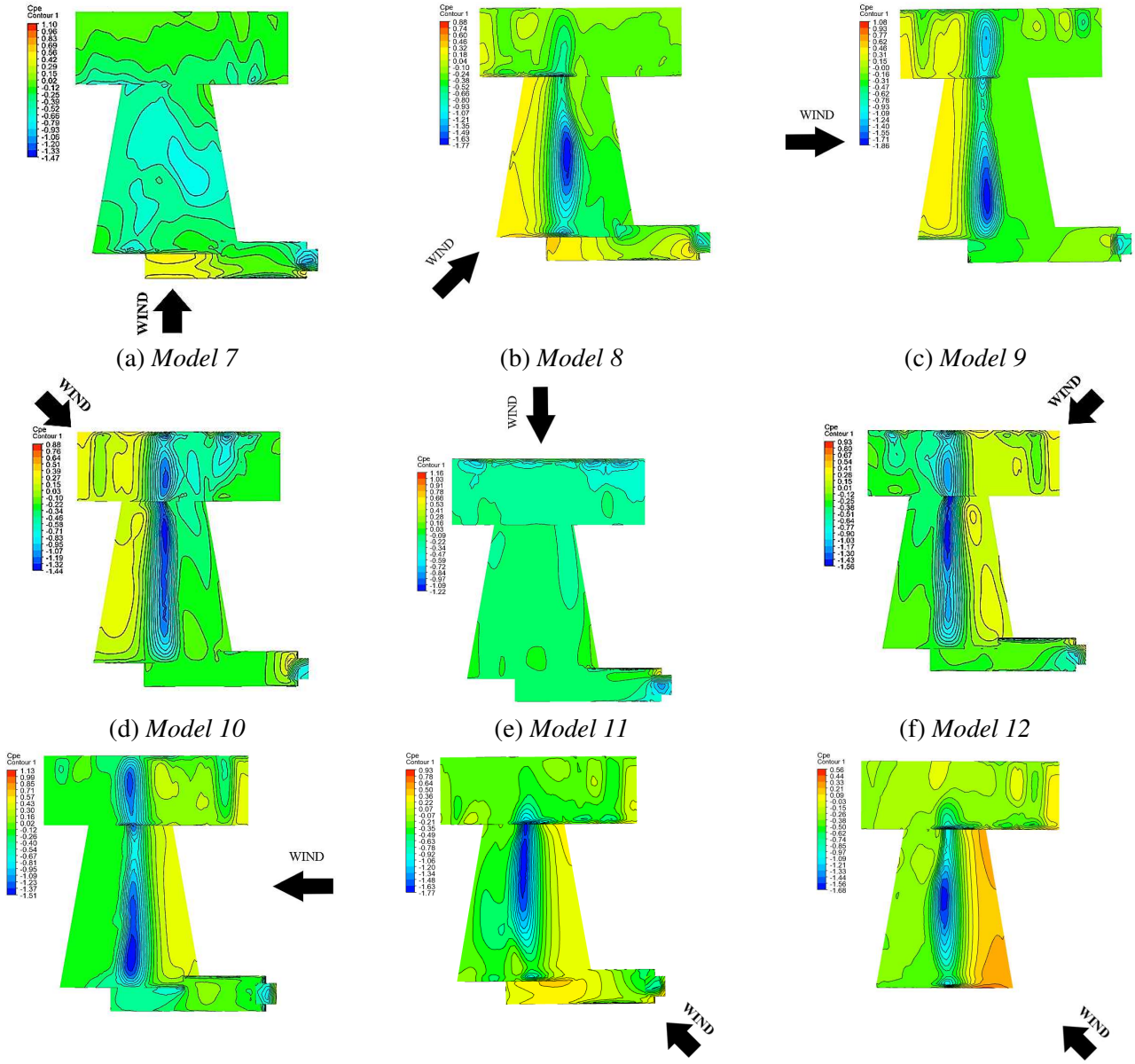

(a) *Model 7* (b) *Model 8* (c) *Model 9*

(d) *Model 10* (e) *Model 11* (f) *Model 12*

(g) *Model 13* (h) *Model 14* (i) *Model 15*

Fig. 8 Separation of overpressure and suction zones.

Table 6. Results of *Model 15* with their respective quality metrics.

Model	*Direction*	*Nodes*	*Elements*	*Element quality (average)*	*Skewness (average)*	*Orthogonal quality (average)*
15	315°	115680	656071	0.81684	0.25258	0.74638

However, a small amount of fluid accelerates past the tower bell, reaching 25 m/s. On the other hand, downstream of the architectural element, the color scale indicated values close to zero. The disturbed flow quickly returns to 14 m/s, returning to the initial configuration, before reaching the main dome shell (A in Fig. 1). This behavior was repeated for the 3.5 m and 5 m levels (Fig. 9b-c), with their respective speed variations. Thus, these architectural elements caused a small local change in the flow. Their positions and geometric configurations allowed the fluid to regain its initial characteristics before generating effects on the parabolic coverage.

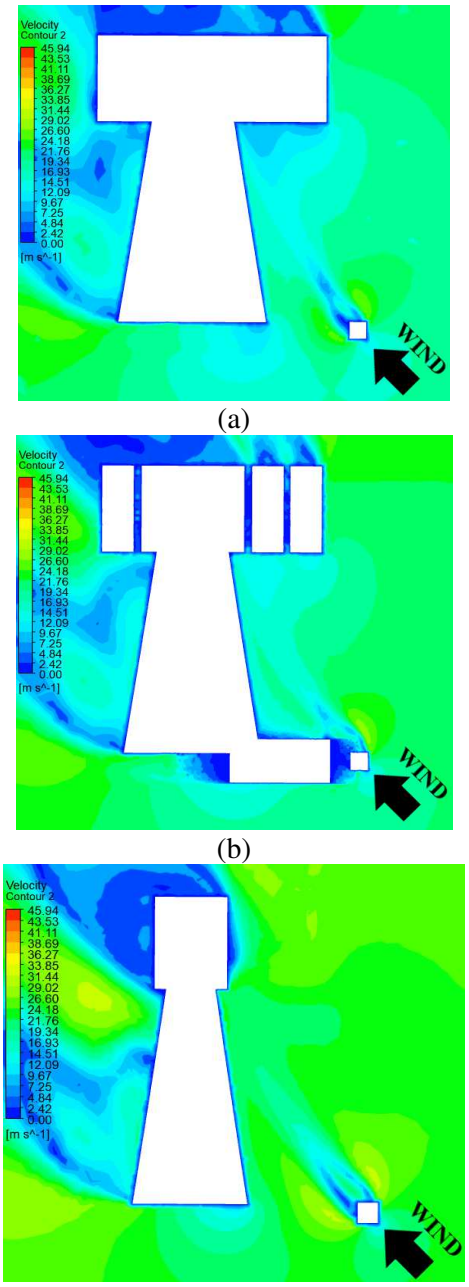

(a)

(b)

(c)

Fig. 9 Ground-parallel velocity contours for *Model 15*, assuming heights of (a) 2 m, (b) 3.5 m, and (c) 5 m.

4 Conclusions

This paper used computational studies in wind action analyses in an innovative project composed of parabolic and circumferential generatrices: the *Church of Saint Francis of Assisi*, designed by Brazilian architect Oscar Niemeyer in Belo Horizonte, Brazil.

The numerical simulations were carried out on significant regions of the paraboloid roof using *Ansys Workbench* software.

This work investigated the pressure coefficient with numerical tests on seven different geometries of hyperbolic paraboloid roofs.

In the flow, eight wind angles of attack (0°, 45°, 90°, 135°, 180°, 225°, 270°, and 315°) and architectural elements (bell tower and marquee) were considered.

The validation methodology considered two hyperbolic paraboloid roofs with square plan models. The maximum difference of 0.4 occurred in the suction of the hyperbolic paraboloid.

For the various directions of wind incidence under the Church of Saint Francis of Assisi simulated, the parabolic cover presented similar behavior in the two situations.

In the first one, the wind orthogonally reached the main facades (front and back). The pressure coefficient contours were distributed uniformly, without great values for peaks (in the absolute values).

In the second, the wind flowed directly or partially on the sloping concrete roofs, showing significant detachment points and a clear separation between the suction and overpressure regions.

In general, the directions 45°, 135°, 225°, 270°, and 315° were considered unfavorable.

The results showed that the marquee and bell tower caused a low local disturbance in the flow, which was not enough to generate high effects on the structure.

In this case, with or without the presence of architectural elements, the maximum difference in the external pressure coefficients was 0.1.

Finally, these results can motivate the elaboration of a roadmap to reduce the accidents in buildings due to wind. Furthermore, to fill the material gap for scholars in the area, the effects of wind on paraboloid roofs should be reduced.

Other works may study the remaining wind directions and the internal pressure coefficients. In the critical regions, one could analyze the existence of crack openings and their connection with the action of the winds. Finally, the effects on the structure due to the vortices caused by the steeple interception in the flow are determined.

References:

[1] J. A. Schultz and V. Henriksson, Structural assessment of St. Charles hyperbolic paraboloid roof, *Curved and Layered Structures*, Vol. 8, 2021, pp. 157–166.

[2] Y. Qiu, Y. Sun, Y. Wu, B. San and Y. Tamura, Surface roughness and Reynolds number effects on the aerodynamic forces and pressures acting on a semicylindrical roof in smooth

flow, *Journal of Structural Engineering*, Vol. 144, No. 9, 2018, 04018140.
[3] M. Lazzari, A. V. Saetta and R. V. Vitaliani, Non-linear dynamic analysis of cable-suspended structures subjected to wind actions, *Computers and Structures*, Vol. 79, No. 9, 2001, pp. 953–969.
[4] F. Rizzo and V. Sepe, Static loads to simulate dynamic effects of wind on hyperbolic paraboloid roofs with square plan, *Journal of Wind Engineering and Industrial Aerodynamics*, Vol. 137, 2015, pp. 46–57.
[5] F. Rizzo, P. D'Asdia, M. Lazzari and L. Procino, Wind action evaluation on tension roofs of hyperbolic paraboloid shape. *Engineering Structures*, Vol. 33, No. 2, 2011, pp. 445–461.
[6] F. Rizzo, P. D'Asdia, F. Ricciardelli and G. Bartoli, Characterization of pressure coefficients on hyperbolic paraboloid roofs. *Journal of Wind Engineering and Industrial Aerodynamics*, Vol. 102, 2012, pp. 61–71.
[7] J. Xu, Y. Zhang, L. Zhang, M. Wu, Y. Zhou, K. Lei and Q. Zhang, Wind-induced response of open type hyperbolic-parabolic membrane structures, *Structural Engineering and Mechanics*, Vol. 76, No. 2, 2020, pp.269-278.
[8] F. Rizzo and C. Demartino, Pressure modes for hyperbolic paraboloid roofs, *Curved and Layered Structures*, Vol. 7, 2020, pp.226-246.
[9] B. Rong, S. Yin, Q. Wang, Y. Yang, J. Qiu, C. Lin and R. Zhang, Simulation and analysis of wind pressure coefficient of landslide-type long-span roof structure, *Advances in Civil Engineering*, Vol. 2021, 2021, p. 1-15.
[10] M. L. M. A. Sousa, F. L. Carsalade, R. Z. Araújo, O reconhecimento dos valores patrimoniais pela comunidade e o conjunto moderno da Pampulha, *Arquitecturas del Sur,* Vol. 40, No. 61, 2022, pp. 8-23.
[11] D. M. Macedo, *Da matéria à invenção: As obras de Oscar Niemeyer em Minas Gerais, 1938-1955,* Câmara dos Deputados, 2008 (in Portuguese).
[12] J. Franke, A. Hellsten, H. Schlünzen and B. Carissimo, *Best practice guide for the CFD simulation of flows in the urban environment, COST Action 732: Quality assurance and improvement of microscale meteorological models,* COST Office, 2007.
[13] M. R. Such, *Análise aerodinâmica de um veículo de eficiência energética,* Undergraduate thesis, Federal University of Santa Catarina, 2018 (in Portuguese).
[14] J. Franke, C. Hirsch, A. G. Jensen, H. W. Krüs, M. Schatzmann, P. S. Westbury, S. D. Miles, J. A. Wisse and N. G. Wright, *Recommendations on the use of CFD in predicting pedestrian wind environment , COST Action C14: Impact of Wind and Storms on City Life and Built Environment. Hamburg*, COST Office, 2004.
[15] Inc. ANSYS, *ANSYS CFX-Solver Modeling Guide*. Canonsburg, 2009.
[16] H. S. Santana, A. G. P. Silva, M. G. M. Lopes, A. C. Rodrigues, O. P. Taranto and J. L. Silva Jr, Computational methodology for the development of microdevices and microreactors with ANSYS CFX, *MethodsX,* Vol. 7, 2020, 100765.
[17] M. T. Vallis, *Brazilian Extreme Wind Climate,* Doctoral dissertation, Federal University of Rio Grande do Sul, 2019 (in Portuguese).
[18] J. Blessmann, *O vento na Engenharia Estrutural*, UFRGS, 2013 (in Portuguese).

Contribution of individual authors to the creation of a scientific article

Guilherme Teixeira was responsible for the methodology, carrying out the simulation, and writing the results. Marco Campos carried out the conceptualization, review, and editing.

Creative Commons Attribution License 4.0 (Attribution 4.0 International , CC BY 4.0)